

Swash zone dynamics of a sandy beach with low tide terrace during variable wave and tide conditions

Luis Pedro ALMEIDA¹, Rafael ALMAR¹, Patrick MARCHESIELLO¹,
Rachid BENSILHA¹, Kevin MARTINS², Chris BLENKINSOPP², France FLOC'H³,
Jeromme AMMANN³, Philippe GRANDJEAN⁴, Nguyen VIET⁴, Duong THUAN⁴,
Le BINH⁵, Nadia SENECHAL⁶, Guillaume DETANDT⁶, Melanie BIAUSQUE⁶,
Thierry GARLAN⁷, Erwin BERGSMA⁸, Charles CAULET³, Hai-Yen TRAN⁹

1. Laboratoire d'Etudes en Géophysique et Océanographie Spatiales, 18, av. Edouard Belin, 31401 Toulouse cédex 9, Toulouse, France.
luis.pedro.almeida@legos.obs-mip.fr
2. University of Bath, United Kingdom.
3. Université Bretagne Occidentale, Brest, France.
4. Hanoi Water Resources University, Hanoi, Vietnam.
5. Hydraulic Engineering Consultants, Hanoi, Vietnam.
6. EPOC - Université de Bordeaux, France.
7. Service Hydrographique et Océanographique de la Marine, Brest, France.
8. Plymouth University, United Kingdom.
9. Laboratoire des Écoulements Géophysiques et Industriels, Grenoble, France.

Abstract:

A field experiment was conducted on a sandy beach with a low tide terrace (Nha Trang, Vietnam) to investigate the swash zone hydro- and morphodynamics throughout different tide and wave conditions. A 2D Lidar was used to measure runup properties and bed level changes on the swash zone. An energetic monsoon wave event provided energetic conditions during the initial stage of this experiment while mild wave conditions were observed during the remaining days. Swash dynamics were clearly modulated by wave and tide conditions. Preliminary results indicate that wave climate is linked with extreme runup and beach erosion and recovery processes while tide level seems to affect swash spectral signature (dominated by infragravity band during low tide and incident band during high tide) and linked with asymmetrical morphological response of the swash.

Keywords: Swash zone, Wave runup, Morphological changes, Remote sensing.

1. Introduction

The swash is composed of two distinct phases, an upslope, landward directed, flow (uprush) and a downslope, seaward directed flow (backwash). Although there is a continuum of energy in swash spectra, they are commonly divided into incident ($f > 0.05$ Hz) and infragravity frequencies ($f < 0.05$ Hz). The incident band is normally

more energetic in bore-dominated, steeper intermediate and reflective beaches (RAUBENHEIMER & GUZA, 1996), while low sloped dissipative beaches have been observed to have most of the swash variance within infragravity frequencies (RUGGIERO *et al.*, 2004). Beaches with steep upper slope sand flat low-tide terraces (LTT) represent a special case where the three distinct hydrodynamic regimes (reflective, intermediate and dissipative) can be observed at different tide stages (MILES & RUSSELL, 2004). Tide modulation of the wave breaking processes on the surf zone (*e.g.*, plunging breakers at high tide breaking on the steeper section of the profile; spilling breakers during low tide breaking on the LTT), are expected to affect significantly the hydro- and morphodynamics of the swash zone of these environments, although with the exception of some studies on mixed sand and gravel beaches (*e.g.*, MILES & RUSSELL, 2004, or KULKARNI *et al.*, 2006), these processes have not been investigated on sandy environments. The aim of the present work is to investigate the swash zone hydro- and morphodynamics on a sandy beach with a steep upper slope and flat LTT, during variable wave and tide conditions.

2. Methods

2.1 Study site

A field experiment was undertaken between 26 November and 04 December 2015 at Nha Trang beach, a sandy beach located on a semi-closed bay on the South East of Vietnam (Figure 1). This medium-to-coarse sandy beach ($D_{50} = 0.3$ mm) has a fairly steep beach face slope (~ 0.1) and a narrow (~ 40 m) alongshore uniform and flat (~ 0.01) low tide terrace (LTT). The beach is a mixed wave-dominated micro-tidal environment (Relative Tidal Range, RTR ~ 1), with a mixed to diurnal tide. The site selected for this field experiment is located at the North region of Nha Trang beach (Figure 1), in a region sheltered from SE winds and waves by Tre, Mieu and Tam islands. Apart from extreme events such as Typhoons (typically from North direction) the beach is for most of the time under local generated SE wind-waves with moderate energy, and Monsoon swells from NE direction, responsible for dominant South-North long-shore sediment transport.

2.2 Field measurements

Swash zone hydrodynamics and morphological evolution were measured using one high frequency video camera HD (Sony HDR-CX 250) and 11 buried metallic poles painted in black (Figure 1). This method allows the collection of time series of high frequency (at 25 Hz) water surface elevation and bed level at each pole. A 2D Lidar (SICK LMS500) deployed on the top of a metallic tower (Figure 1) was used with the same propose, however providing an higher spatial resolution and range (distance between

points of about 1 cm and maximum cross-shore range of about 30 meters each side of the scanner) than the swash video pole method.

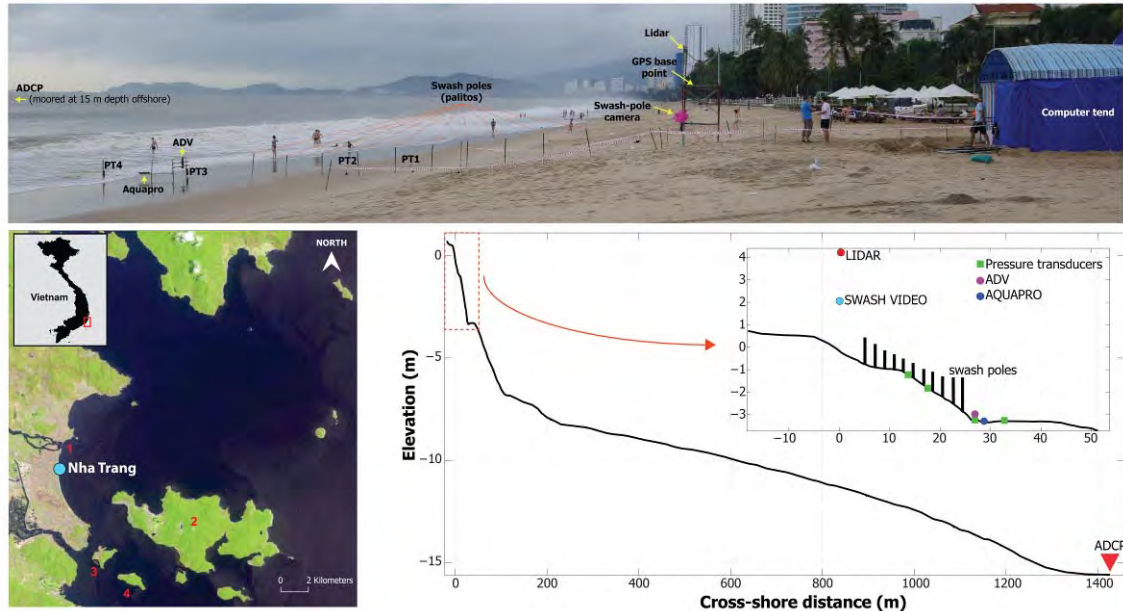


Figure 1. Location of Nha Trang beach (left bottom map) with the indication of the experiment site (blue dot) and some important local features: 1 - Cai river; 2 - Hon Tre island; 3 - Hon Mieu island; 4 - Hon Tam island. Panoramic photo of the cross-section of the field experiment (top photo) showing the location of each instrument, and beach profile (full and zoom in the experiment region - bottom right) with the position of the instruments referred to the local coordinate system ($x, y=0$ at the GPS base point).

In addition to these two remote sensing instruments (video and Lidar), one scaffold rig with one ADV (Nortek), one current profiler (Nortek - Aquapro) and one self-logging pressure transducer was installed on the inner part of the LTT, just at the intersection with the lower beach face (Figure 1). Three other self-logging pressure transducers were installed between the LTT and the upper beach face (Figure 1). Offshore wave characteristics were recorded by an ADCP that was moored offshore at 15 m depth to (Figure 1). To complement this dataset of measurements topographic surveys were performed at every low tide (using RTK-GPS equipment) and covering an area of 600 m to each side of the main instrument profile. Survey were performed in a continuous mode (recording every 0.5 m) along cross-shore transects spaced by 10 m. In the present work are only presented results relative to the ADCP and Lidar observations.

2.3 Hindcast wave conditions during the experiment

A regional wave hindcast for the experimental period was performed using WAVEWATCH III (TOLMAN, 2002). Previous WW3 applications in the South China

Sea (SCS) have been validated against buoys and altimeter data (e.g., MIRZAEI *et al.*, 2013). Here, a WW3 configuration is implemented to simulate SCS wave characteristics from November 18th to December 5th 2015. The computational domain covers the area from 95°E to 150°E and 5°S to 35°N at 0.25° resolution. Its extension to the Northwest Pacific Ocean encompasses the main zone of tropical cyclone intensification. The bathymetric data was obtained from ETOPO2 at 2-min resolution (~3 km). The wind forcing data is interpolated from the archived 0.5-degree, 6-hourly analysis product from the Global Forecast System of the National Center for Environmental Prediction (NCEP, NOAA).

3. Results and Discussion

3.1 Hindcast wave conditions

A set of results from WW3 simulations is presented in Figure 2, covering from the 26-11-2015 to 28-11-2015, and it shows that during the beginning of this experiment an energetic swell event propagated into SCS from NE direction.

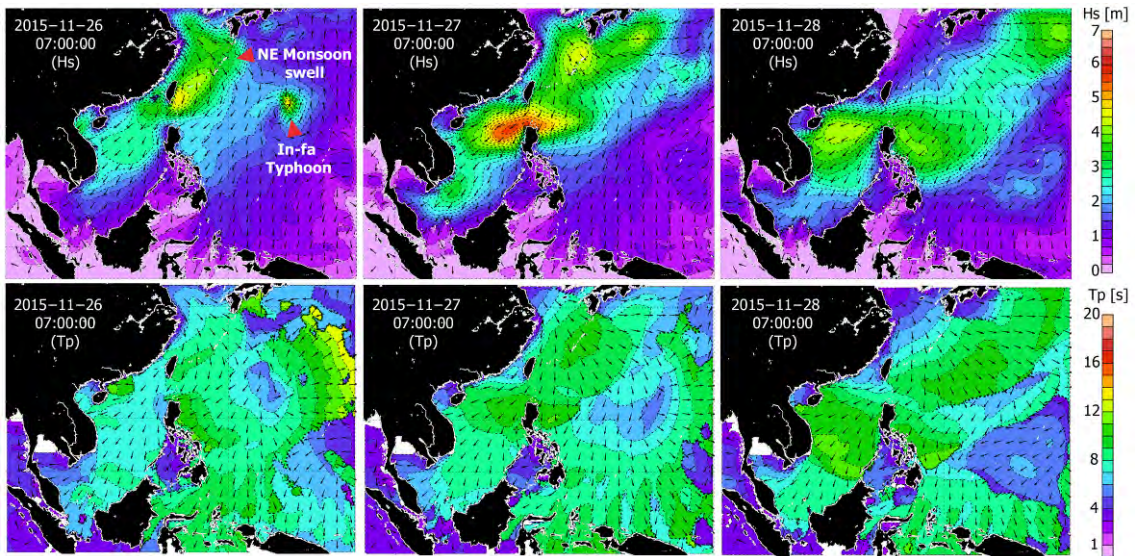


Figure 2. WW3 hindcast results (*Hs* and *Tp*) for the 26, 27 and 28 of November 2015.

This event represents a typical winter Northeast monsoon storm, although with an apparent initial strengthening due to the presence of a tropical Typhoon (In-Fa - category 4 typhoon that occurred on the Philippines sea between 16 to 27 November 2015) at the initial stages of this storm (Figure 2).

3.2 Offshore wave conditions and tides

The comparison of these WW3 simulations with the offshore wave measurements performed by the ADCP show a good agreement, despite the difference of the H_s magnitude which is likely to be due to the local effects of the bathymetry and shadowing by some small islands that is not detailed in these model simulations.

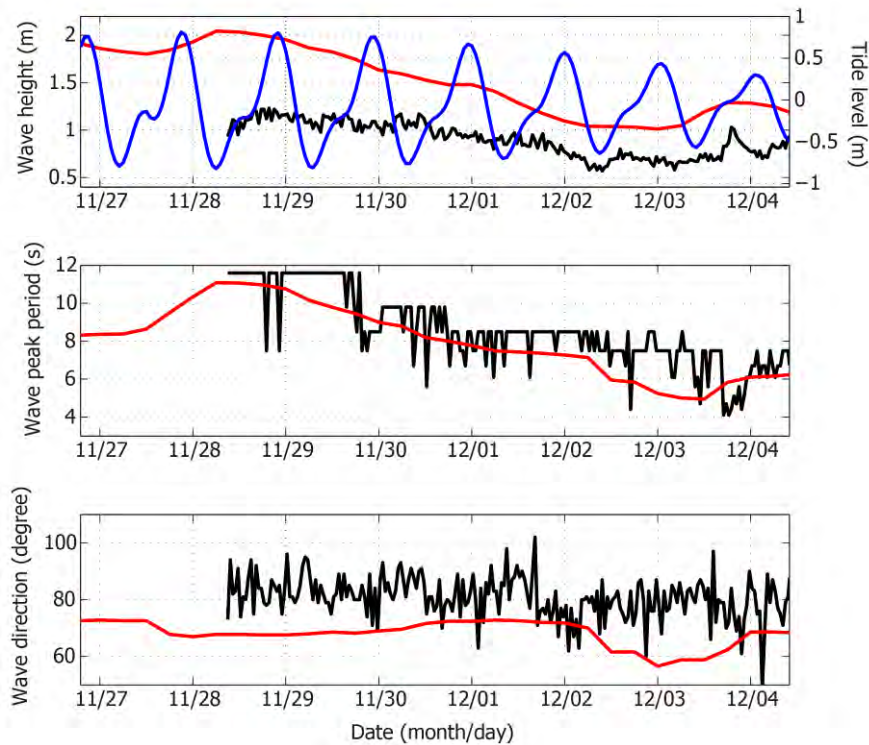


Figure 3. Offshore wave measurements performed with the ADCP (black line) with the overlap of the WW3 hindcast results (red line) and predicted tide (blue line – predictions were made using WX Tide software). Top panel shows the significant wave height (H_s), middle panel the wave peak period (T_p) and bottom panel wave direction.

The wave conditions during this experiment were significantly distinct. While during the first days of the experiment (from the 27 until the 30 Nov 2015) an energetic wave event with large offshore H_s (~ 2 m predicted by WW3 and ~ 1.3 m measured by the ADCP) and T_p (between 8 and 12 seconds) was observed, in remaining days of the experiment the wave conditions become milder (Figure 3). Beyond the waves, also the tide range decreased during the experiment period, from approximately 1.5 m to 0.75 m.

3.3 Swash hydrodynamics and morphological response

Swash hydrodynamics of Nha Trang beach were investigated through the calculation of the 2% exceedance of the vertical runup maxima ($R2\%$) and runup spectra for continuous segments of 20 minutes of measurements following the approach of

STOCKDON *et al.* (2006). Results show a clear link between the R2% and the offshore wave conditions (Figure 4). The highest R2% coincide with the peak of offshore wave heights and the largest wave periods (29-11-2015), while the lowest values of R2% coincide with the mildest wave conditions (Figure 4).

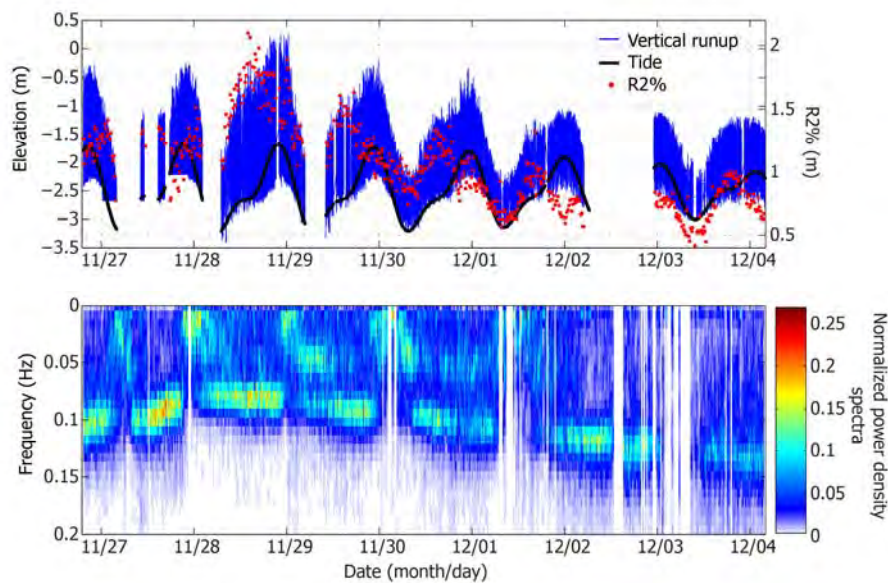


Figure 4. Time series of runup elevation (blue line) with the overlap of the predicted tide (black line) and R2% (red dots – top panel); vertical runup spectra, normalized by total energy (bottom panel).

Significant different spectral signature of the vertical runup was found between low and high tide conditions (Figure 4) with low tide showing that most of the energy is on the infragravity band ($f < 0.05$ Hz) while with the rising tide the energy gradually becomes concentrated on the incident band with the peak of energy coinciding with the peak period of the offshore incident waves measured at the ADCP. Such distinct spectral signature at different tide stages suggests a strong link to the differential wave dissipation processes. During low tide the LTT exhibits characteristics very similar to an dissipative beach, with large wave dissipation occurring along the full extension of the terrace, promoting a swash zone dominated by the energy of long period spilling bores, contrasting with high tide where waves reach the inner surf zone unbroken and dissipate most of their energy near the lower beach face (MILES & RUSSELL, 2004). The morphological feedback of the swash zone under such distinct hydrodynamic forcing was also investigated using the Lidar measurements. Time averaged (computed for consecutive segments of 10 minutes) beach profiles were used to compute the cumulative vertical changes for the entire duration of the experiment (Figure 5). Results show that during the initial days of the experiment (under energetic wave conditions) erosion was observed in the upper part of the beach resulting from berm erosion (Figure

5). In the following days and under mild wave conditions it was observed that the beach developed significant recovery, with the formation of a new berm with a crest slightly lower than the previous existing one (Figure 5).

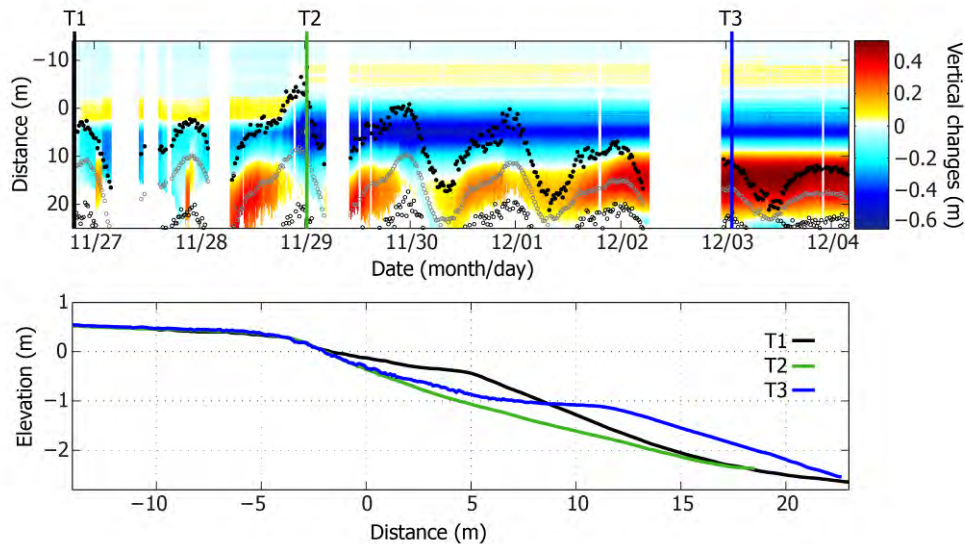


Figure 5. Morphological response of the beach during the Nha Trang experiment, with the cumulative vertical changes (top panel), and the overlap of the initial, middle and final beach profiles observed during this experiment (bottom panel).

The cumulative changes also provide interesting insights on the morphological response of the swash zone during the tide cycle, with asymmetrical morphological changes (accretion during rising and erosion during falling tide) occurring in most of the tides (Figure 5). Similar morphological response has been observed on mixed sand and gravel beaches with LTT (*e.g.*, KULKARNI *et al.*, 2004) or steep pure gravel beaches during energetic wave conditions (ALMEIDA *et al.*, 2015) however on sandy beaches with LTT such response was not observed before. Such morphological response is likely to be linked with the tide modulated swash hydrodynamics (*e.g.*, wave breaking processes), but also could be a result of the complex feedback processes between morphology (*e.g.*, slope) and hydrodynamics. Further analysis will be performed in order to investigate which are the fundamental processes underlying these distinct swash morphodynamics.

4. Conclusions

The swash zone dynamics of a sandy beach with a LTT (Nha Trang, Vietnam) was investigated under different tide and wave conditions. Preliminary results show that with larger offshore waves the extreme vertical runup (R2%) is higher than during mild wave conditions. Tide modulation of the wave breaking on the LTT has a profound

Thème 2 – Dynamique sédimentaire

impact on the swash hydrodynamics. During low tide waves dissipate their energy mostly on the LTT and swash zone is dominated by infragravity wave runup excursions while during high tide waves dissipate their energy closer to the shore and swash is dominated by incident band. These preliminary results show that swash morphological response have a direct relationship with offshore wave climate, with energetic waves promoting erosion (*e.g.* berm erosion) and mild waves promoting accretion (*e.g.* berm formation). New insights on the swash asymmetrical morphological response during a tide cycle are presented here for the first time on sandy beach and further work will be performed to investigate the link between this morpho response and the hydrodynamics.

5. Acknowledgments

This research has received support from French grants through ANR (COASTVAR: ANR-14-ASTR-0019).

6. References

- ALMEIDA L.P., MASSELINK G., RUSSELL P., DAVIDSON M. (2015). *Observations of gravel beach dynamics during high energy wave conditions using a laser scanner*. *Geomorphology*, Vol. 228, pp 15-27. <http://dx.doi.org/10.1016/j.geomorph.2014.08.019>
- MIRZAEI A., TANGANG F., JUNENG L, MUSTAPHA M.A., HUSAIN M.L., AKHIR M.F. (2013). *Wave climate simulation for southern region of the South China Sea*. *Ocean Dynamics*, Vol. 63(8), pp 961-977.4. <http://dx.doi.org/10.1007/s10236-013-0640-2>
- KULKARNI D., LEVOY F., MONTFORT O., MILES J. (2004). *Morphological variations of a mixed sediment beachface (Teignmouth, UK)*. *Continental Shelf Research*, Vol. 24(11), pp 1203–1218. <http://dx.doi.org/10.1016/j.csr.2004.03.005>
- MILES J., RUSSELL P. (2004). *Dynamics of a reflective beach with low tide terrace*. *Continental Shelf Research*, Vol. 24(11), pp 1219-1247. <http://dx.doi.org/10.1016/j.csr.2004.03.004>
- RAUBENHEIMER B., GUZA R.T. (1996). *Observations and predictions of run-up*. *Journal of Geophysical Research*, Vol. 101(C11), pp 25575–25587. <http://dx.doi.org/10.1029/96JC02432>
- RUGGIERO P., HOLMAN R.A., BEACH R.A. (2004). *Wave run-up on a high-energy dissipative beach*. *Journal of Geophysical Research*, Vol. 109(6), pp 1-12. <http://dx.doi.org/10.1029/2003jc002160>
- STOCKDON H.F., HOLMAN R.A., HOWD P.A., SALLENGER Jr. H. (2006). *Empirical parameterization of setup, swash and runup*. *Coastal Engineering*, Vol. 53, pp 573–588. <http://dx.doi.org/10.1016/j.coastaleng.2005.12.005>
- TOLMAN H.L. (2002). *Validation of WAVEWATCH III version 1.15 for a global domain*. NCEP/NOAA/NWS, National Centers for Environmental Prediction, Technical note 213, Washington.